 UK-UNLIMITED

(2)

AD-A205 650

ARE TM(UHA) 88512

ARE TM(UHA) 88512

October 1988

COPY No. 21

COMPARISON OF INTEGRAL AND FINITE-DIFFERENCE METHODS FOR PREDICTING THE TURBULENT BOUNDARY LAYER ON AXISYMMETRIC BODIES

D. J. ATKINS

REPORTS QUOTED ARE NOT NECESSARILY AVAILABLE TO MEMBERS OF THE PUBLIC OR TO COMMERCIAL ORGANISATIONS

ADMIRALTY RESEARCH ESTABLISHMENT
Procurement Executive, Ministry of Defence
Queens Road, Teddington, Middlesex

UK-UNLIMITED

COMPARISON OF INTEGRAL AND FINITE-DIFFERENCE METHODS FOR PREDICTING THE TURBULENT BOUNDARY LAYER ON AXISYMMETRIC BODIES

by

D J ATKINS

Summary

Predictions of the attached turbulent boundary layer on three axisymmetric bodies were obtained using integral and finite-difference methods. The integral method was developed by Myring and the finite-difference method by Wang & Huang. Both methods take account of viscous-inviscid interaction effects and the finite-difference method also takes account of the variation of static pressure across the boundary layer. Comparisons with experimental data show both methods to be of similar accuracy over all but the last few per cent of the body length. However, the finite-difference method is marginally superior in this region and gives more detailed information, including the individual velocity components and the Reynolds shear stress.

22 pages
9 figures

ARE (Teddington)
Queen's Road
Teddington Middx TW11 0LN

August 1988

C O N T E N T S

LIST OF SYMBOLS

C_f	Skin-friction coefficient = (wall shear stress)/$\frac{1}{2}\rho U_e^2$
H	Shape factor = $\Delta^\star/\Theta$
L	Body length
R0	Body radius at axial distance X from nose
R	Radial distance from axis
U,V	Tangential and normal components of mean velocity
U',V'	Tangential and normal turbulent velocity fluctuations
U_e	Velocity at edge of boundary layer
UINF	Freestream velocity
UX,UR	Axial and radial components of mean velocity
X	Axial distance from nose
Y	Normal distance from body surface
α	Angle of tangent to body surface with respect to axis
δ	Boundary layer thickness
$\delta^\star$	Boundary layer displacement thickness
$\Delta^\star$	Displacement area = $\int_0^\delta (1-U/U_e)\ (R0 + Y\cos\alpha)\ dY$
θ	Momentum area = $\int_0^\delta U/U_e(1-U/U_e)\ (R0 + Y\cos\alpha)\ dY$

INTRODUCTION

Current ARE propulsor design methods for underwater vehicles require a knowledge of the boundary layer flow in the region of the propulsor on the unpropelled vehicle. A typical vehicle configuration often comprises a non-axisymmetric hull shape fitted with control fins, which results in a highly three-dimensional flow field with vortex shedding and high levels of turbulence. Although such flow fields can be measured on scale models, the Reynolds numbers involved are usually considerably lower than the full-scale value, sometimes by a factor of 100. However, axisymmetric calculation methods can be used to give design information and estimate the boundary-layer Reynolds number scaling effects.

An integral method for predicting the turbulent boundary layer on axisymmetric bodies, developed by Myring [1], has been in use at ARE for several years. The method was designed primarily for predicting drag and has been shown to give good results for a wide variety of body shapes [2]. There is also reasonable agreement with experiment of the boundary-layer integral parameters and velocity profiles, which are required for propulsor design purposes, on body shapes with small longitudinal curvature and tail cone semi-angles of less than about 20°. For body shapes with fuller sterns, the agreement is less favourable with the shape parameter in particular being under-predicted at the tail end of the body where the boundary layer may be close to separation.

The present investigation aims to compare the Myring method with a more sophisticated finite-difference method developed by Wang & Huang [3,4,5] and described in Section 2 below. Accurate measurements of the boundary-layer velocity components and Reynolds stresses using hot-wire or laser-Doppler anemometry are now available, and these are compared in Section 3 with predictions using both integral and finite-difference methods for three representative body shapes.

2. THEORY

Both the integral and the finite-difference method use the same technique based on the displacement body concept, i.e. the static pressure or velocity at the edge of the boundary layer (required by the boundary-layer calculation) is the same as the surface pressure or velocity in an inviscid flow over the body surface to which the displacement thickness has been added. This means that the boundary-layer and potential-flow calculations can be coupled together in an iterative cycle. The potential calculation in both methods is based on the source panel method of Hess & Smith [6]. The main difference between the two methods is in the boundary-layer calculation. In the finite-difference method the momentum equation is solved directly, whereas in the integral method it is formally integrated across the boundary layer to give the momentum integral equation, which is then solved empirically.

The Myring integral method proceeds as follows: the boundary layer is calculated using an initial guess at the external pressure distribution. The location of transition to turbulence must be prescribed explicitly by the user. The potential flow is then calculated over the "displacement surface" and the predicted pressure distribution is used as the input to the next boundary-layer calculation. The calculation is extended into the wake and suitable end conditions are imposed. The profile drag is estimated from the momentum deficit in the far wake and the skin-friction drag by integrating the local skin-friction coefficient over the body surface. An iterative scheme results which stops when the iterated values of drag have converged, usually after about six iterations. Profiles of the tangential velocity along a normal to the hull can be determined by assuming a power-law profile. The method has been adapted to include a simple actuator-disk representation of a lightly-loaded propeller [7].

The Wang & Huang method is based on the finite-difference solution of the boundary-layer equations developed by Cebeci & Smith [8]. The location of transition can be prescribed or predicted using a simple empirical method, and the effects of a tripping device can be incorporated. A simple eddy-viscosity model of turbulence is used, which is based on the traditional mixing-length approach. The flow in the wake is calculated using an integral method proposed by Granville [9]. The displacement surface is determined from the boundary-layer and wake calculations, but in the body stern and near-wake regions a fifth-degree polynomial is used to connect the two displacement surfaces. The iteration procedure starts with a potential flow calculation over the body surface, and continues until the maximum change in the pressure coefficient on the displacement surface is less than a specified tolerance, or the number of iterations is exceeded. The results converge in an oscillatory manner, and so the final pressure coefficient is usually taken to be the average of the previous two values. The original version of the method has been improved in two ways [5]. Firstly, a correction was made to the predicted velocity profiles to take account of the variation of static pressure across the boundary layer and to obtain the correct conditions at the freestream boundary. Secondly, the turbulent mixing-length formulation was modified to include thick boundary-layer effects. Both modifications are aimed at giving improved predictions in the propulsor region at the stern of the body.

3. COMPARISON OF THEORY WITH EXPERIMENT

In this Section, brief details are given of boundary-layer measurements on three axisymmetric bodies, and the measurements are compared with integral and finite-difference method predictions. The body shapes are a prolate spheroid with conical tail, which was investigated by Patel et al [10], and two in-house bodies: a torpedo-shaped body with an inflected stern, known as the propulsor research vehicle (PRV) [11] and a body with a streamline nose and tail cone with 15-degree semi-angle [12]. Figure 1 shows the geometry and notation in the thick boundary

layer near the tail of a typical body, and the body shapes actually used are plotted as Figure 2.

The modified spheroid was investigated experimentally by Patel et al [10] in a low speed wind tunnel at Iowa Institute of Hydraulic Research. The tunnel speed was 40 ft/sec (12.2 m/s) corresponding to a body-length Reynolds number of 1.26×10^6. Velocity and Reynolds stress measurements were conducted using a hot-wire anemometer, with the boundary-layer traverses being normal to the hull enabling direct comparison with boundary-layer calculation methods. In the present investigation, predictions of the boundary-layer integral parameters and velocity profiles were obtained using both integral and finite-difference methods. Figures 3 and 4 show comparisons with theory of the measured integral parameters derived by integrating the velocity measurements across the boundary layer. Figure 5 shows comparisons of the tangential and normal velocity components as predicted by the integral and finite-difference methods with hot-wire measurements. The integral method can only predict the tangential component. The finite-difference predictions here do not take into account the variation of static pressure across the boundary layer. The integral method predictions agree well with the measurements for $X/L \leq 0.93$. At $X/L=0.99$, the finite-difference method is clearly superior to the integral method in predicting the tangential velocity component. Figure 6 shows similar comparisons with experiments of finite-difference predictions, both uncorrected and corrected to allow for static pressure variation across the boundary layer. The improvement between the uncorrected and corrected profiles is only marginal for the tangential velocity component, but is more significant for the normal velocity component, particularly near the edge of the boundary layer. Figure 7 shows measurements and finite-difference predictions of the Reynolds shear stress. The agreement is good up to $X/L=0.90$ but then falls off. This illustrates the difficulty of using a simple eddy-viscosity model of turbulence in a thick axisymmetric boundary layer.

The propulsor research vehicle has a nose flat and both prediction methods were modified slightly to account for this. Velocity measurements were carried out in the ARE 30-inch Water Tunnel at Teddington at a tunnel speed of 11 m/s corresponding to a body length Reynolds number of 3×10^7. The body diameter was 0.324m and the tunnel has a slotted wall working section 0.76m in diameter, so there may have been some small blockage effect. Boundary-layer velocity components were measured using a two-axis laser-Doppler system. Two traverses were undertaken, one moving in a horizontal direction, where the axial and radial components were measured, and the other in a vertical direction, where the axial and circumferential components were measured. The turbulence levels were also estimated, but these were found to be relatively high because of the slotted wall.

The measurements of axial and radial velocity components are compared with finite-difference predictions in Figure 8. The measured profiles are along radii and the predictions along normals to the hull. However examination of the predictions suggest that the velocity profiles do not change significantly in

the distance spanned by the measured boundary layer and so no correction was applied. The finite-difference method is shown to give reasonable predictions of both the axial and radial velocity components.

The body with the 15-degree tail cone was tested in the No 5 Wind Tunnel at British Maritime Technology Ltd. at a body length Reynolds number of 6.5×10^6. The main objective of the experiments was to study the wake of a body with fins, but some preliminary measurements were carried out on the unappended body. The axial and radial velocity components were measured traversing the boundary layer along a radius. The measurements were taken at one axial and seven radial locations and a complete circumferental traverse was obtained at 1° intervals. The purpose of this experiment was to ensure that any departures from axial symmetry due to the effects of the supporting strut and wires were minimal. Axial velocities were measured traversing in a radial direction. These are compared with finite-difference predictions in Figure 9 and the agreement is generally favourable.

4. CONCLUSIONS AND FURTHER RESEARCH

The Wang & Huang finite-difference and Myring integral methods for predicting the turbulent boundary layer on axisymmetric bodies have been evaluated against each other and compared with experiment. The methods are found to be of similar accuracy over all but the extreme tail end of a practical body shape. However the finite-difference method is marginally superior in this region because it takes some account of static pressure across the boundary layer. The integral method can only predict the tangential velocity component, whereas the finite-difference method can predict the tangential and normal or axial and radial components and the Reynolds shear stress. However the integral method is easier to use and produces much less output than the finite-difference method. The finite-difference method is recommended for the majority of future computations, but some preliminary calculations, for example, to investigate the effect of varying a parameter, are probably best performed using the integral method.

There are several more sophisticated axisymmetric body prediction methods now available and a review of these has recently been carried out by Patel & Chen [13]. For our current body shapes they appear to be only marginally more accurate than the finite-difference method but require significantly more computational effort. For practical vehicle configurations including control fins and propulsor, a three-dimensional Reynolds-averaged Navier-Stokes calculation is necessary. Research into the relevant numerical methods is now in progress at ARE.

D J Atkins (SSO)

REFERENCES

1. MYRING, D.F. The profile drag of bodies of revolution in subsonic axisymmetric flow. Royal Aircraft Est TR72234 (1973).

2. ATKINS, D.J. Assessment of a method for predicting the drag and boundary-layer development on a body of revolution at zero incidence. Admiralty Marine Technol Est AMTE(N)R78111 (1979).

3. HUANG, T.T. et al. Propeller/stern/boundary-layer interaction on axisymmetric bodies: theory and experiment. DTNSRDC Rep 76-0113 (1976).

4. WANG.H.T. & HUANG.T.T. User's manual for a FORTRAN IV computer program for calculating the potential flow/ boundary-layer interaction on axisymmetric bodies. DTNSRDC SPD-737-01 (1976).

5. WANG, H.T. & HUANG, T.T. Calculation of potential flow/ boundary-layer interaction on axisymmetric bodies. Proc. ASME Symp. on Turbulent Boundary Layers, Niagara Falls, N. Y. (1979).

6. HESS, J.L. & SMITH, A.M.O. Calculation of potential flow about arbitrary bodies. Progress in Aeronaut Sci, Vol 8, Pergamon Press (1966).

7. ATKINS, D.J. The effect of a propulsor on the hull boundary layer of a body of revolution. Admiralty Marine Technol Est AMTE(N)TM79101 (1979).

8. CEBECI, T. & SMITH, A.M.O. Analysis of turbulent boundary layers. Academic Press (1974).

9. GRANVILLE, P.S. The calculation of the viscous drag of bodies of revolution. David Taylor Model Basin Rep 849 (1953).

10. PATEL, V.C. et al. An experimental study of the thick turbulent boundary layer near the tail of a body of revolution. Iowa Inst of Hydraul Res Rep 142 (1973).

11. ARE Drawing no N1/1161.

12. ARE Drawings nos G/2008/1-6 and N1/1165.

13. PATEL, V.C. & CHEN, H.C. Flow over tail and in wake of axisymmetric bodies: review of the state of the art. J Ship Res 30(3)201-214 (1986).

Reports quoted are not necessarily available to members of the public or to commercial organisations.

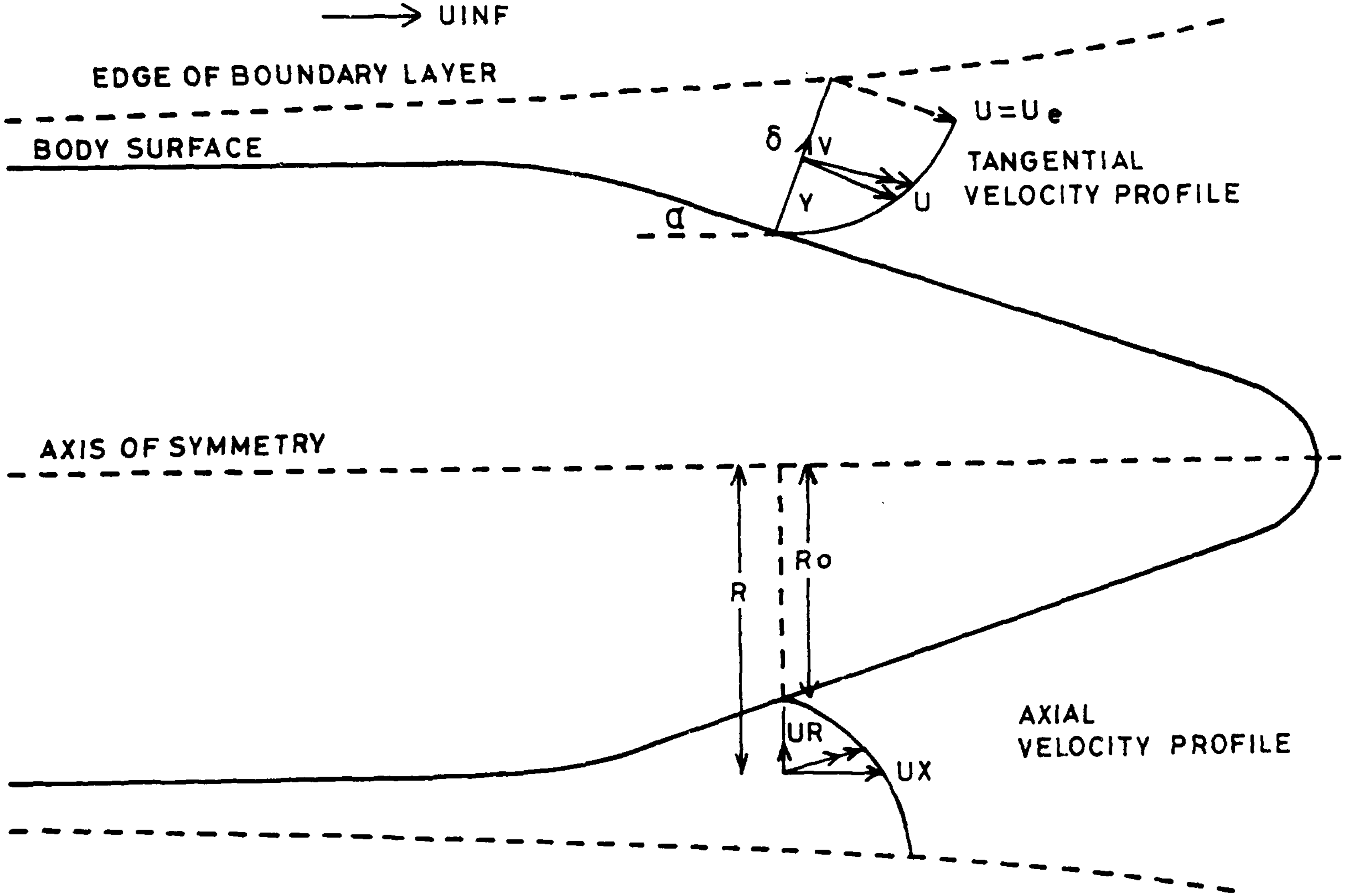

FIG.1 BODY GEOMETRY AND NOTATION

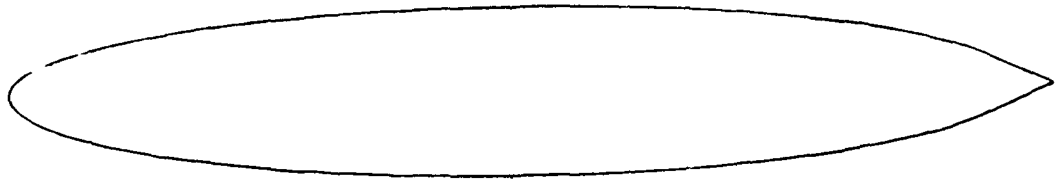

(a) MODIFIED SPHEROID

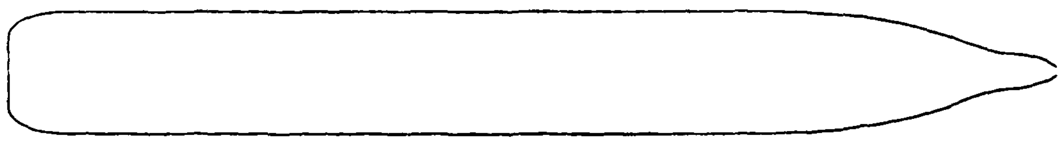

(b) PROPULSOR RESEARCH VEHICLE

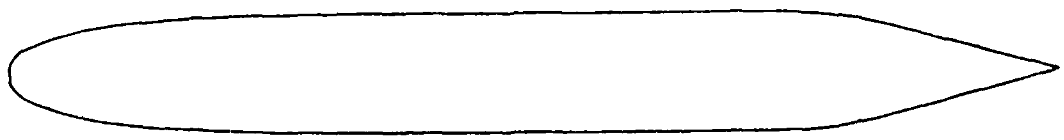

(c) BODY WITH 15 DEG. TAIL CONE

FIG. 2 BODY SHAPES TO SCALE

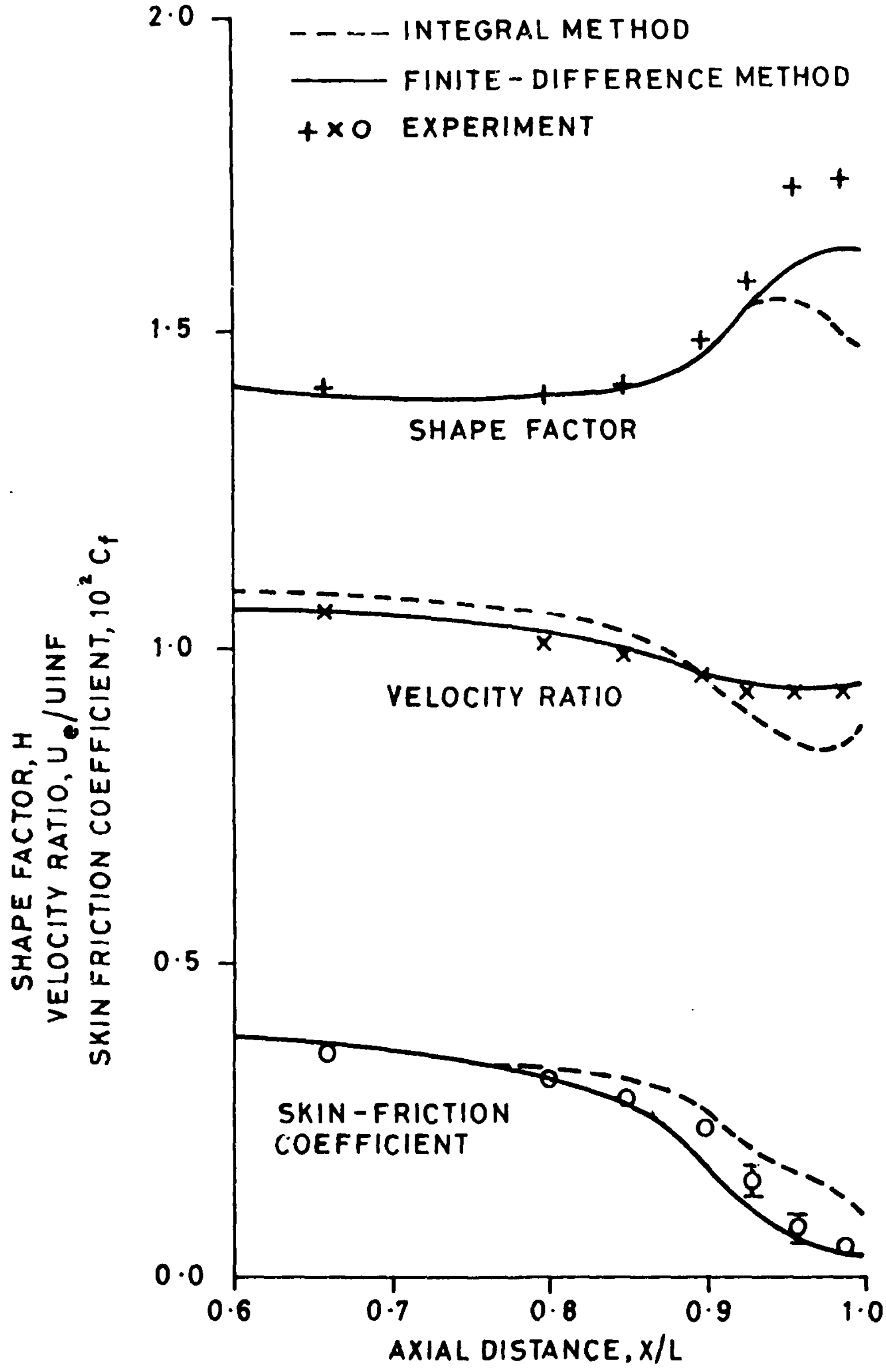

FIG.3 COMPARISON OF PREDICTED AND MEASURED BOUNDARY LAYER PARAMETERS FOR MODIFIED SPHEROID

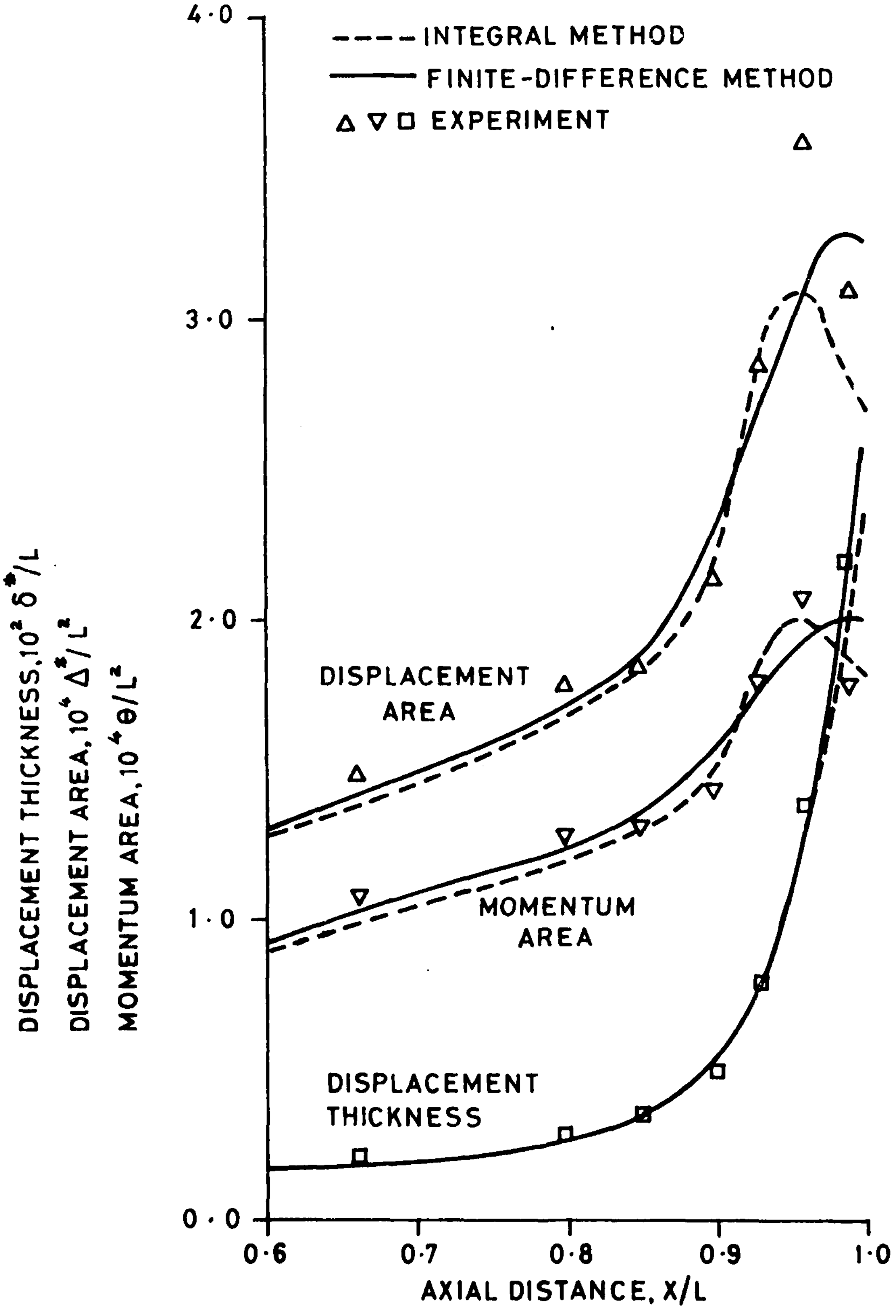

FIG4 FURTHER COMPARISON OF PREDICTED AND MEASURED BOUNDARY LAYER PARAMETERS FOR MODIFIED SPHEROID

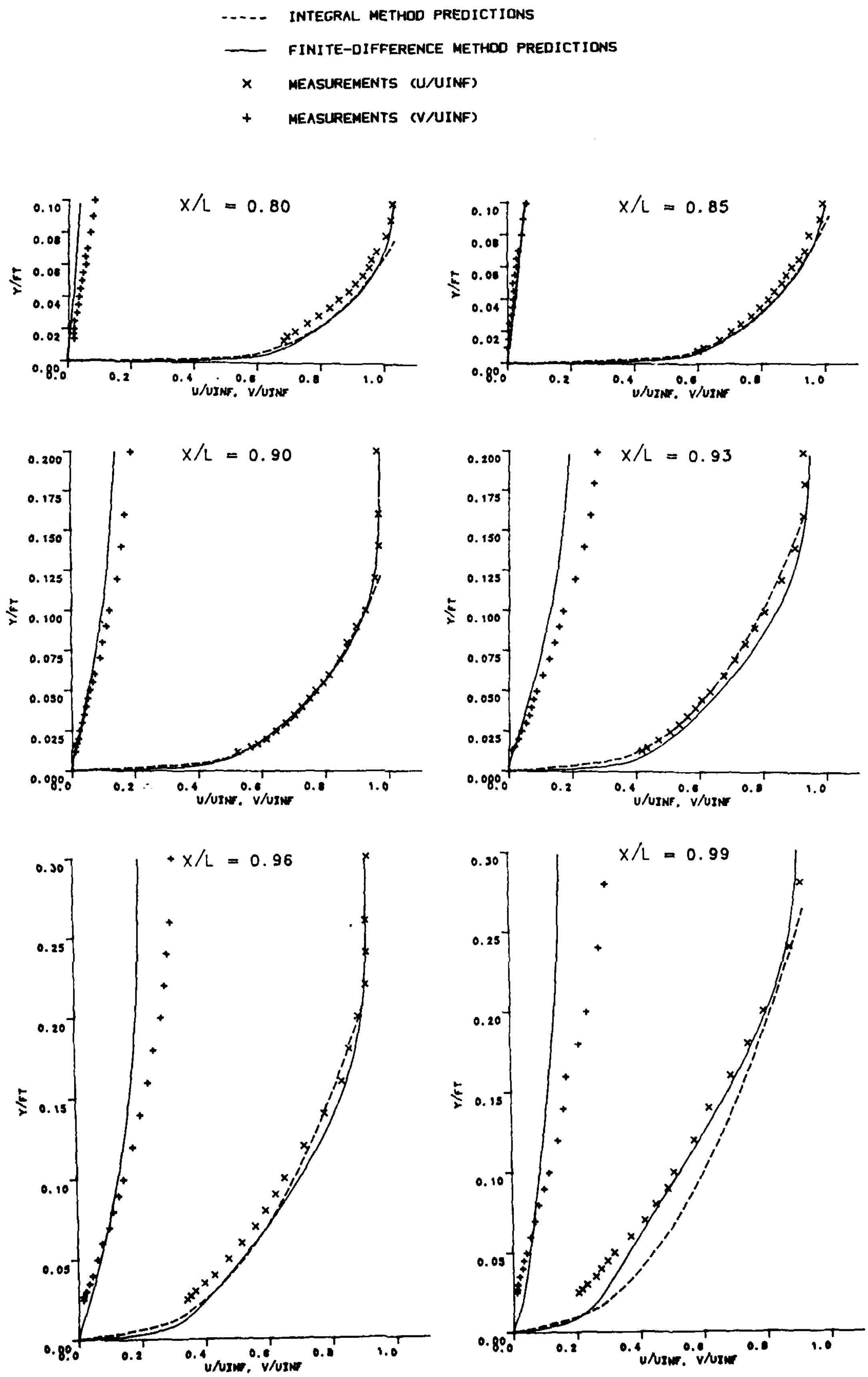

FIG. 5 COMPARISON OF PREDICTED AND MEASURED TANGENTIAL AND NORMAL VELOCITIES ON MODIFIED SPHEROID

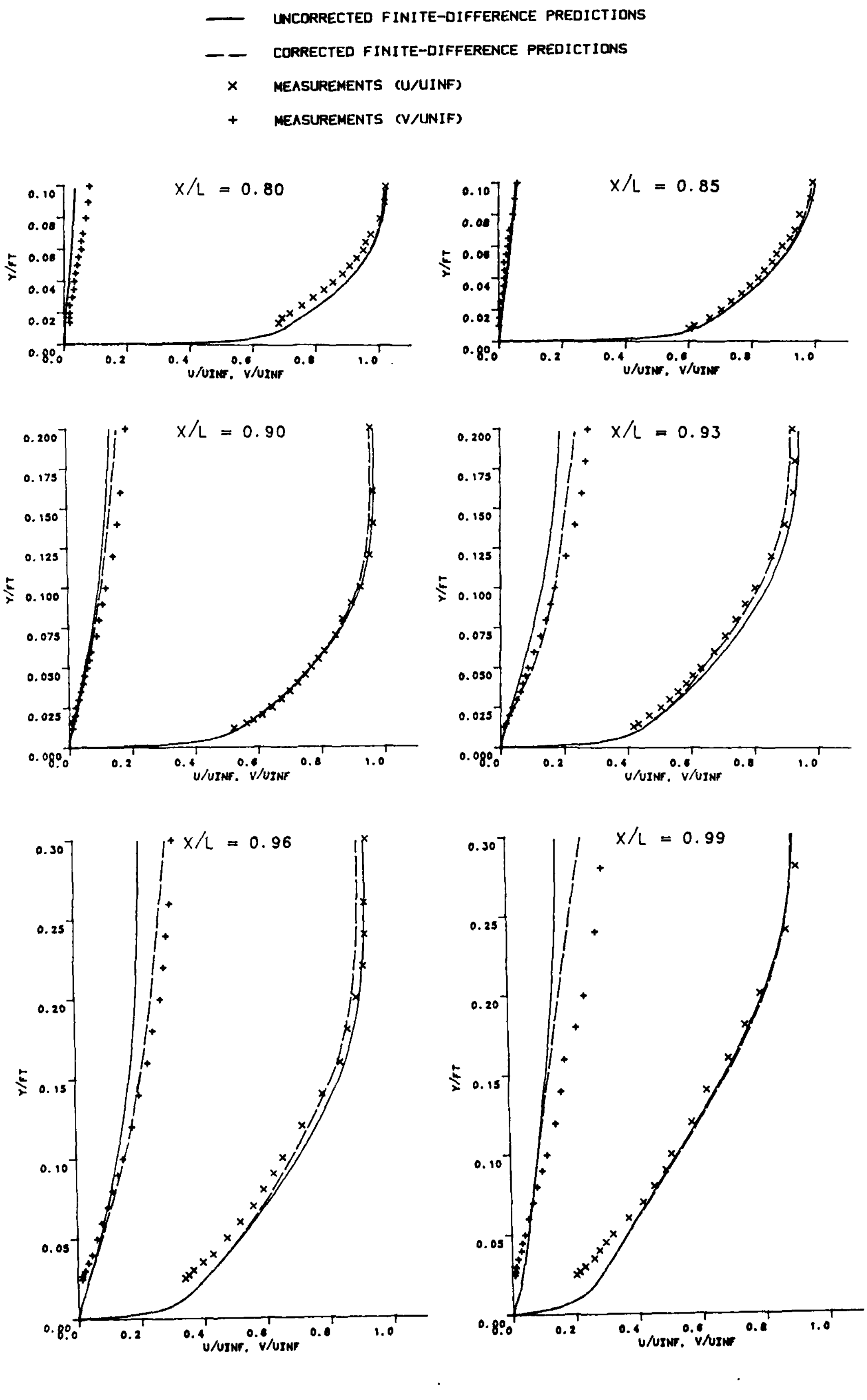

FIG. 6 COMPARISON OF FINITE-DIFFERENCE PREDICTIONS AND MEASUREMENTS SHOWING EFFECT OF STATIC PRESSURE CORRECTION (MODIFIED SPHEROID)

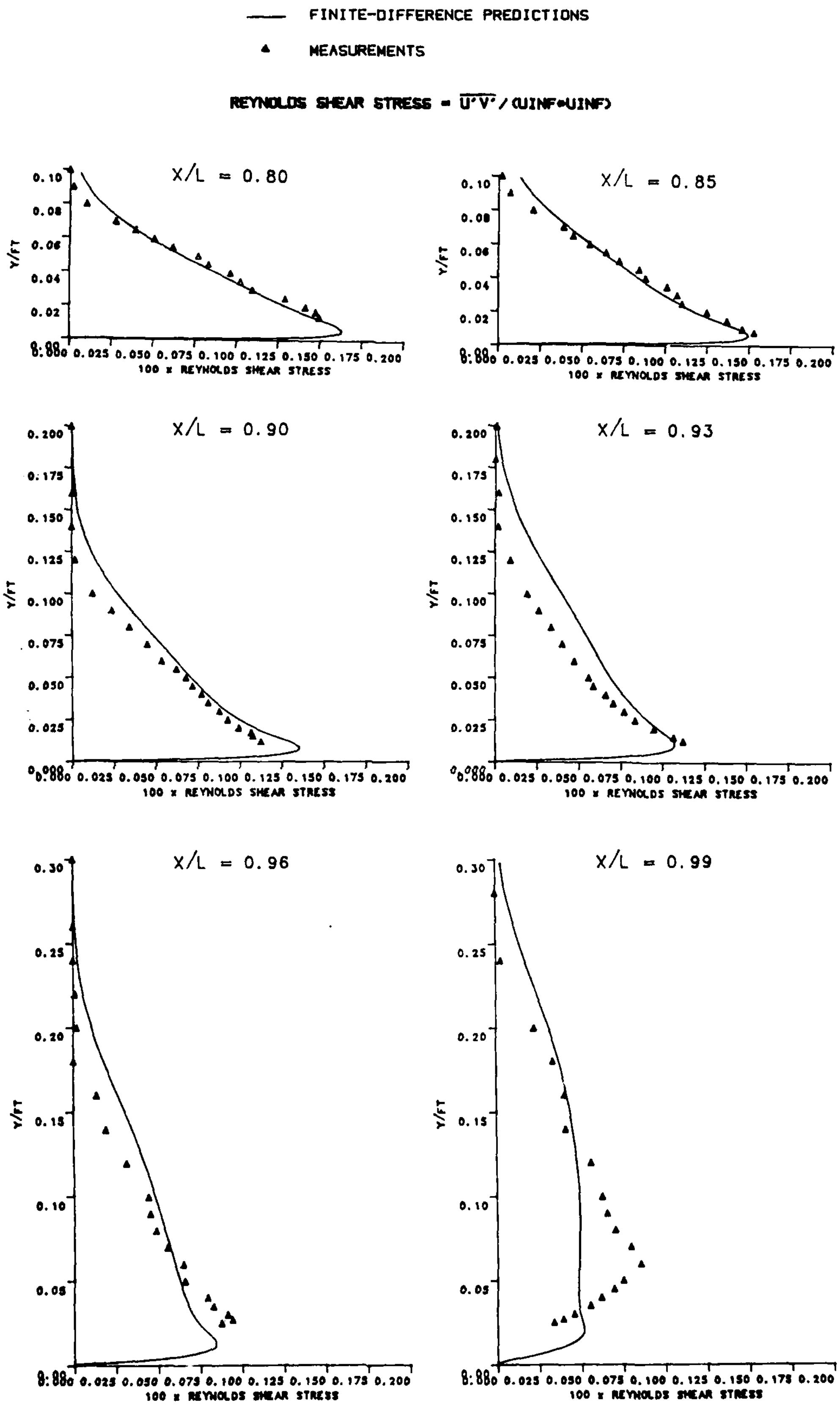

FIG. 7 COMPARISON OF PREDICTIONS AND MEASUREMENTS OF REYNOLDS SHEAR STRESS ON MODIFIED SPHEROID

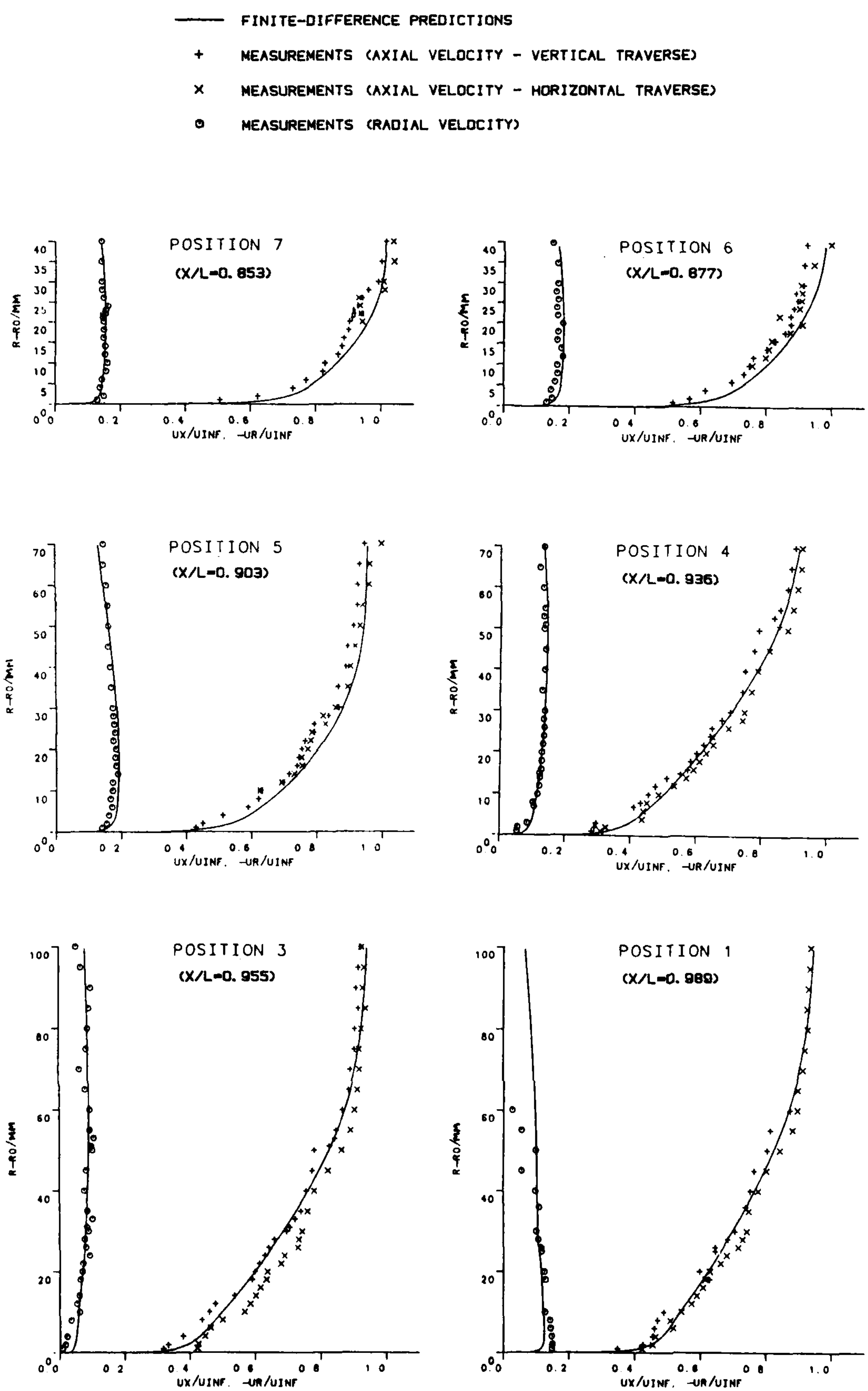

FIG. 8 COMPARISON OF PREDICTED AND MEASURED AXIAL AND RADIAL VELOCITIES ON PROPULSOR RESEARCH VEHICLE

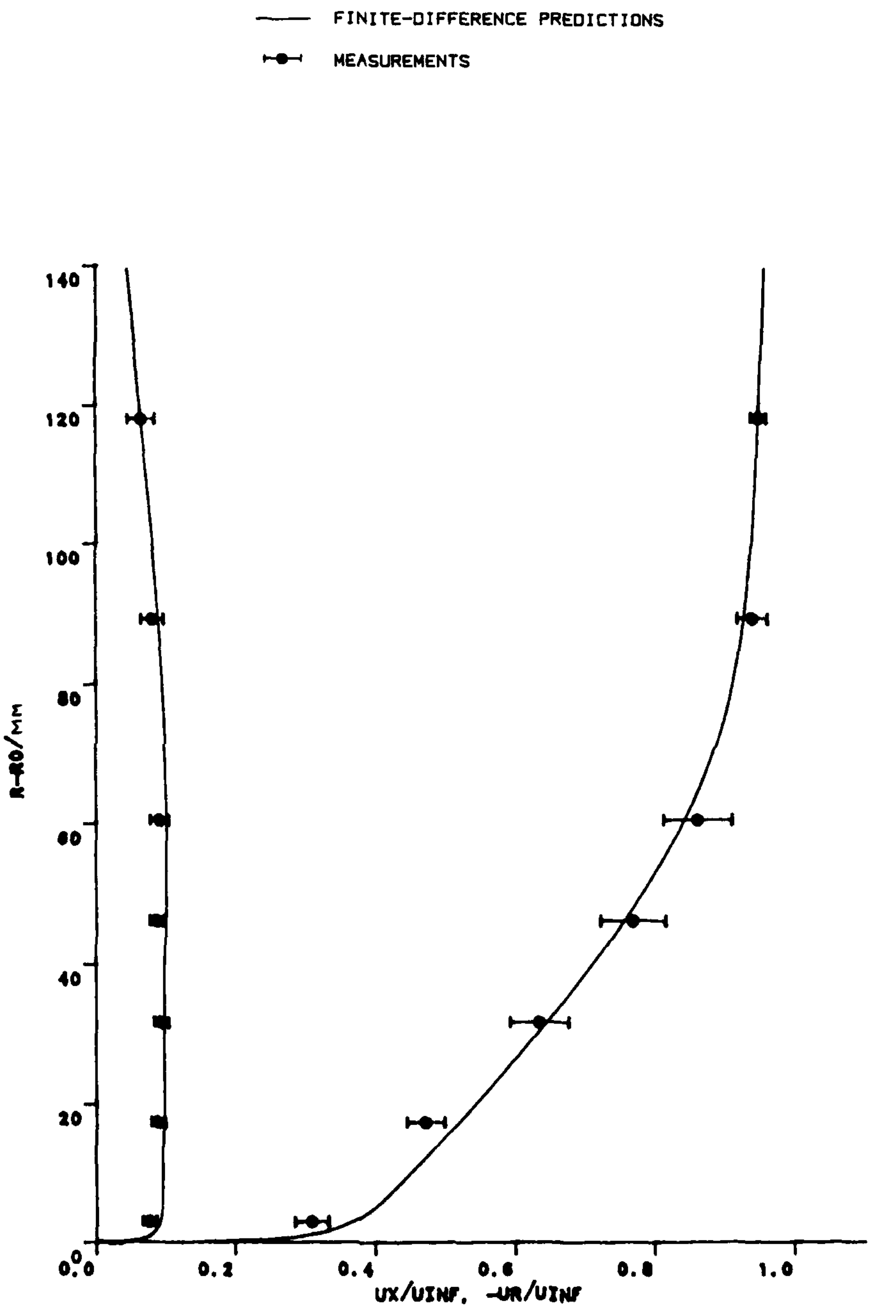

AXISYMMETRIC BODY WITH 15 DEGREE TAIL CONE

FIG. 9 COMPARISON OF PREDICTED AND MEASURED AXIAL AND RADIAL VELOCITIES

DISTRIBUTION

	Copy No
D Sc (Sea)	1
DD(U) ARE (Portland)	2
DES Washington	3
CS (R) 2e Navy	4
ARE (Haslar) UH	5
ARE (Haslar) UHR	6
ARE (Haslar) UHU	7
ARE (Portland) UDU	8
ARE (Portland) UTW	9
DRIC	10-39
IEP ABC-17	40-45
RAE (Farnborough) Library	46
ARE (Haslar) Technical Information Centre	47-55